

Electron dephasing in wurtzite indium nitride thin films

Z. W. Jia and W. Z. Shen^{a)}

Laboratory of Condensed Matter Spectroscopy and Opto-Electronic Physics, Department of Physics, Shanghai Jiao Tong University, 1954 Hua Shan Road, Shanghai 200030, People's Republic of China

H. Ogawa and Q. X. Guo

Department of Electrical and Electronic Engineering, Faculty of Science and Engineering, Saga University, Saga 840-8502, Japan

(Received 23 June 2006; accepted 22 October 2006; published online 4 December 2006)

The authors present magnetotransport measurements of electron dephasing characteristics in wurtzite indium nitride thin films grown by metal-organic vapor phase epitaxy. Pronounced weak antilocalization effects have been observed at low magnetic fields due to the presence of strong spin-orbit interactions at the top of the valence band. With the aid of the weak localization theory, they are able to demonstrate that the dephasing is connected to three separate processes of the spin-orbit, electron-phonon, and extended structural defect scatterings. The spin-orbit splitting has been determined to be 5.7 meV. They have also shown that both the magnetoresistivity and resistivity can be explained using the same temperature-dependent dephasing times. © 2006 American Institute of Physics. [DOI: 10.1063/1.2400097]

As a promising semiconductor material among group III-nitride compounds, indium nitride (InN) has recently attracted intensive research interest. However, many of its fundamental properties are still not clearly known despite detailed investigations since the 1980s. In addition to the argument on the energy band gap,^{1,2} the spin-orbit splitting of the top valence band in InN is also controversial, with the theoretical values varying from 1 to 13 meV.³ As we know, spin-orbit splittings have played a very important role in elucidating the band structure of semiconductors⁴ and in investigating the control of spin relaxation rate for spintronics.⁵ Usually, low temperature reflection measurements have the ability to reveal the spin-orbit splittings in semiconductors; nevertheless, there is no optical report up to now to clarify this issue in InN.

In fact, the easy realization of *n*-type InN with very high electron concentrations provides an experimental basis for investigating in detail the electron dephasing in InN, since the magnetotransport study has been demonstrated to be a powerful probe into the electron dephasing with very reliable and quantitative estimations over a wide range of temperature and disorder. The electron dephasing time is a quantity of fundamental interest and importance in semiconductors and metals. It is now widely accepted that weak localization and electron-electron interactions are both crucial to determine the transport properties of electrons in disordered metals and highly degenerate semiconductors.⁶

The phase of two complementary electron waves traveling along a closed path in opposite directions remains coherent unless an inelastic scattering mechanism or an external magnetic field breaks the time-reversal symmetry. The quantum corrections of the localization effects to the classic Boltzmann magnetoresistivity (MR) can be negative or positive depending on the importance of the spin-orbit scatterings at the top of the valence band in the studied materials. In the presence of strong spin-orbit scatterings, the constructive in-

terference, which gives rise to the localization with negative MR, turns to destructive interference instead, i.e., weak antilocalization, where the magnetic-field-induced electron dephasing results in positive MR phenomenon.⁷ In contrast, the quantum corrections of the electron-electron interactions to the MR are always positive, and arise predominantly from Zeeman splitting of the spin-up and -down electrons.

In *n*-type materials, spin-orbit scatterings originate from the scattering of conduction electrons off heavy impurities and/or surfaces. The existence of indium clustering in high electron concentration InN (Ref. 8) will result in strong spin-orbit scatterings, which have been revealed in the temperature-dependent resistivity of InN as a function of carrier density.⁹ According to the weak localization predictions, the presence of strong spin-orbit scattering makes the extraction of electron dephasing times extremely reliable.¹⁰ Therefore, a detailed investigation of the weak antilocalization effects in InN can bring interesting information concerning the role of the spin-orbit interactions, inelastic scatterings, and other factors associated with the electron dephasing processes.

The hexagonal InN thin film for the present study was grown on a (0001) α -Al₂O₃ substrate by microwave-excited metal-organic vapor phase epitaxy at 500 °C. Details of the growth procedures were given elsewhere.^{1,11} The unintentionally doped InN thin film (thickness of 0.35 μ m) exhibits *n*-type conductivity, with Hall mobility (μ) of 365 (280) cm²/V s and electron concentration (*n*) of 2.8 (3.0) $\times 10^{19}$ cm⁻³ at room (liquid helium) temperature. The MR measurements were performed in the van der Pauw configuration by a dc four-probe method with small indium ohmic electrodes on the corners of the 5 mm square sample. The sample was immersed in a ⁴He cryostat system equipped with a 15 T Oxford Instruments superconductive magnet, where the magnetic-field *B* parallels the sample *c* axis and the measured temperature can be down to 1.4 K. The magnetic field reading accuracy was better than 1%.

Figure 1(a) shows the magnetic-field *B* dependent MR of the InN sample at 2.0 K. It is clear that the MR at high

^{a)} Author to whom correspondence should be addressed; electronic mail: wzshen@sjtu.edu.cn

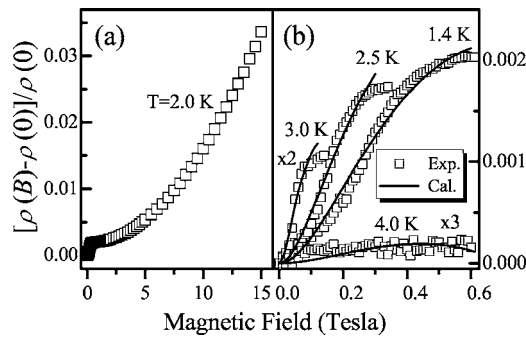


FIG. 1. (a) Magnetic field dependence of the magnetoresistivity in the InN sample at 2.0 K. (b) Low magnetic field magnetoresistivity of the InN sample at various temperatures. Solid curves are the fittings of the weak localization theory with spin-orbit interactions to the experimental data (open squares).

magnetic fields (above 1.0 T) obeys the classical Boltzmann B^2 law, in contrast to the pronounced “anomalous” MR of rapid increase with the magnetic field below 0.6 T. We note that, as Fig. 1(b) displays, the drastic increase in the MR at low magnetic fields can only be observed at temperatures below 4.5 K, and becomes more remarkable with the decrease of temperature. Accordingly, the anomaly has also been found in the temperature dependence of the resistivity [Fig. 2(a)], where we can observe a rapid increase of the resistivity with the temperature below 4.0 K. As we know, the backscattering probability of electrons will be enhanced due to the interference by partial electron waves traveling along time reversed electron path, resulting in the weak localization of the electrons. An externally applied magnetic field suppresses the phase coherence, exhibiting the positive quantum corrections of the MR characteristics at low magnetic fields in heavily doped semiconductors with strong spin-orbit interactions.⁷ We therefore attribute the observed rapid increase of the MR and resistivity to the weak antilocalization effects in InN.

In order to achieve deeper understanding of the weak antilocalization effects in InN, we have performed theoretical calculations to interpret quantitatively the experimental data in Fig. 1(b). The classical MR of the sample is negligible due to $\mu B \ll 1$ in the measured low magnetic fields ($B < 0.6$ T). We have employed Kawabata’s approach to take into consideration the quantum corrections¹² of both the singlet Cooperon (a particle-particle propagator responsible for the quan-

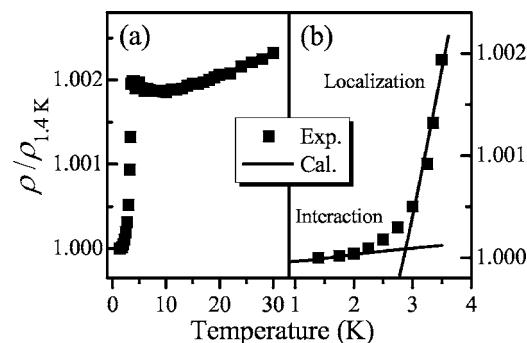


FIG. 2. (a) Temperature dependence of the resistivity in InN between 1.4 and 30.0 K without external magnetic fields. (b) Low temperature resistivity of the InN sample, together with the calculated individual contribution of the weak localization and electron-electron interactions (solid curves) from the localization-interaction model.

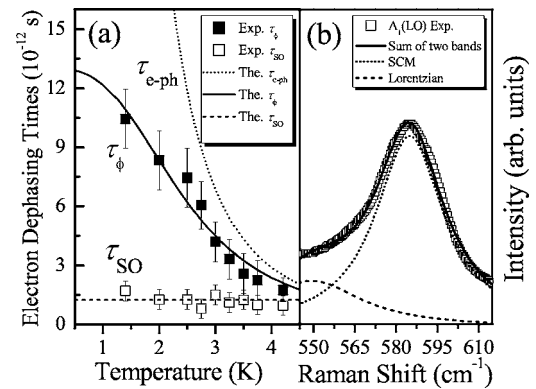


FIG. 3. (a) Temperature dependence of the obtained electron dephasing times in InN from the experimental magnetoresistivity results. (b) Raman spectrum line shape fitting with the SCM (dotted curve) and Lorentzian (dashed curve) for the $A_1(\text{LO})$ phonon mode of the hexagonal InN.

tum interference effect) term containing Zeeman splitting and triplet Cooperon term with spin-orbit scattering. The solid curves in Fig. 1(b) represent the theoretical results, which are in good agreement with the experimental data at various temperatures in the low magnetic field region. There are three parameters in the fitting: the phase coherence time τ_ϕ , the spin-orbit scattering time τ_{SO} , and the classic diffusion coefficient D . Normally, τ_{SO} is a temperature-independent material property.¹⁰ It should be noted that we have not introduced the temperature-dependent prefactor $\alpha(T)$ [$0 < \alpha(T) < 1$] in the quantum corrections, since the magnitude of the MR in InN has already been almost equal to that predicted by the theory.

The scatters in Fig. 3(a) represent the calculated values of τ_ϕ and τ_{SO} by fitting the low magnetic-field MR to the theory at various temperatures. As is seen, the obtained τ_{SO} is nearly constant of $\sim 1.3 \times 10^{-12}$ s (dashed line), in contrast to the clear temperature dependence of τ_ϕ . Furthermore, the spin-orbit scattering rate (τ_{SO}^{-1}) is larger than the electron dephasing scattering rate (τ_ϕ^{-1}) until the high temperature of ~ 4.5 K, where the dephasing scattering rate almost reaches the spin-orbit scattering rate, corresponding to the disappearance of the anomalous MR due to the weak antilocalization effects. It is well known that the D’yakonov-Perel’s (DP) mechanism is the dominant spin relaxation mechanism in disordered systems with strong spin-orbit interactions.⁵ The present InN sample is with high concentration of impurities, where the impurity scattering energy is greater than the spin-orbit splitting value. Scattering leads to “randomization” of the spin states, and τ_{SO}^{-1} turns out to be proportional to the elastic scattering time τ . In this case, we can employ the linear relation between τ_{SO}^{-1} and τ of $\tau_{\text{SO}}^{-1} = \Delta_{\text{SO}}^2 \tau / 2\hbar^2$ in the DP mechanism to determine experimentally the InN spin-orbit splitting of the top valence band Δ_{SO} from the observed weak antilocalization effects. A spin-orbit splitting value of 5.7 meV has been obtained on the basis of the measured τ_{SO} ($\sim 1.3 \times 10^{-12}$ s) and electron mobility (~ 280 cm²/V s) at liquid helium temperature, together with the InN effective mass of $\sim 0.13m_0$ from the electron concentration dependent data of Ref. 13. In III-nitrides, the N 2p component dominates the valence band maximum wave functions, and the semicore cation d states make a negative contribution to Δ_{SO} . The small spin-orbit splitting in InN is due to the light atom of N and considerable hybridization of the N 2p orbital with the In 4d states, where the contribution of the N 2p states is

largely counteracted by that of the In $4d$.⁴ The obtained Δ_{SO} gives a clear experimental support for the recommended value of 5 meV,³ and we are confident that we have clarified the theoretical controversy of 1–13 meV for Δ_{SO} in InN.

It is well known that the main inelastic processes which can cause decoherence in condensed matter electron systems are the electron-phonon, electron-electron, and magnetic impurity interactions. Both the electron-phonon and electron-electron interactions produce a $\tau_{\phi} \sim 1/T^P$ where P varies from 0.5 to 3. At the present studied temperatures (1.4 ~ 4.5 K), the electron-phonon scattering is the dominant inelastic dephasing process in bulk materials with the most easily justified form of $P=3$,¹⁴ though the understanding of the electron-phonon interactions remains incomplete.¹⁰ On the other hand, saturation of the phase coherence time τ_{ϕ} at $T \rightarrow 0$ in the absence of magnetic impurities has been reported,¹⁴ indicating the existence of an additional temperature-independent relaxation mechanism. Zawadowski *et al.*,¹⁵ have proposed an inelastic scattering from two-level centers for such a mechanism. In highly degenerate semiconductors, it is expected that the dangling bonds in the vicinity of grain boundaries will act as the two-level centers. The inelastic scattering is associated with the transmission of the conduction electrons through the potential barriers located at extended structural defects.

We have therefore taken into account the zero-temperature saturation behavior in the analysis of the temperature-dependent phase coherence time τ_{ϕ} : $\tau_{\phi}^{-1} = \tau_{\text{e-ph}}^{-1} + \tau_0^{-1}$, where $\tau_{\text{e-ph}}$ is the electron-phonon inelastic scattering time and τ_0 is the dephasing saturation time. τ_0 can be related to the grain size L_0 by $\tau_0 = L_0^2/D$. The best fit of τ_{ϕ} [solid curve in Fig. 3(a)] does give $P=3$ for the main inelastic electron-phonon process of $\tau_{\text{e-ph}} = 185.2/T^3 \times 10^{-12}$ s, shown as the dotted curve in Fig. 3(a), together with τ_0 of 13.0×10^{-12} s. During the calculation of the quantum corrections in Fig. 1(b), it is found that the diffusion constant D varies from 1.3 to 3.4 cm²/s. The relatively large variation may be partly due to the absence of the temperature-dependent prefactor $\alpha(T)$ in the quantum corrections. We have employed an average value of $D=2.4$ cm²/s to estimate the average grain size presented in the InN sample, which gives L_0 of 56 nm. The smaller grain size, as compared with the film thickness of 350 nm, justifies the employment of three-dimensional weak localization theory to describe the experimental MR in the present work.

The average grain size in InN can also be extracted by the quantitative calculation of the Raman line shape¹⁶ with a spatial correlation model (SCM).^{17–19} The SCM assumes that the phonons can freely propagate in a region with a size of L (correlation length), and will get scattered by the crystal imperfections beyond this area. The correlation length L can be physically interpreted as the average distance between two defects or dislocations or any other kind of imperfections in the crystal, i.e., representing the average grain size L_0 . Figure 3(b) shows the line shape fitting results for the InN A_1 [longitudinal optical (LO)] phonon mode at 585 cm⁻¹, which was recorded in backscattering geometry of $z(x, -)z$ configuration with an Ar⁺ laser (514.5 nm) under a Jobin Yvon LabRAM HR 800 micro-Raman system. We see that the SCM (dotted curve) can achieve a good fitting with an additional weak Lorentzian (dashed curve) in the low frequency side due to the disorder-activated zone edge LO phonons. The

obtained correlation length of 52 nm corresponds well with the average grain size of 56 nm, further confirming the reliability of the above electron dephasing investigation.

Finally, we will show that the rapid increase of the resistivity with the temperature below 4.0 K in Fig. 2(a) can also be interpreted using the weak localization theory with the spin-orbit coupling.¹² As displayed in Fig. 2(b), the localization corrections can well explain the observed resistivity at high temperature (above 2.5 K) with the same temperature-dependent parameters of τ_{ϕ} , τ_{SO} , and D deduced from the MR. Nevertheless, at low temperatures (below 2.0 K), the electron-electron interactions dominates, with the corrections to conductivity exhibiting the dependence of $\sim mT^{1/2}$.⁶ The importance of the electron-electron interactions has also been revealed in the low temperature MR at high (above 10 T) magnetic fields, where the magnetoconductance is found to be proportional to $B^{1/2}$. As the value of m indicates the progress of metal-insulator (Mott) transition, the obtained negative $m = -1.2$ ($\Omega \text{ cm K}^{1/2}$)⁻¹ for the fitting of the measured resistivity below 2.0 K in Fig. 2(b) demonstrates that the present InN sample is deep in the metallic side of the Mott transition. This argument is in accordance with the facts that the InN sample displays the metallic conductivity behavior [i.e., the resistivity increases with temperature above 10 K in Fig. 2(a)], and that the electron density ($\sim 3 \times 10^{19} \text{ cm}^{-3}$) is much higher than the critical carrier density of $2 \times 10^{17} \text{ cm}^{-3}$ for the Mott transition in InN.⁹

This work was supported by the Natural Science Foundation of China under Contract Nos. 10125416, 60576067, and 10674094, the National Minister of Education Program for Changjiang Scholars and Innovative Research Team in University (PCSIRT), the Grant-in-Aid for Scientific Research (c) (No. 16560013) from the Ministry of Education, Culture, Sports, Science, and Technology, Japan, and the Venture Business Laboratory of Saga University.

¹W. Z. Shen, X. D. Pu, J. Chen, H. Ogawa, and Q. X. Guo, *Solid State Commun.* **137**, 49 (2006).

²K. S. A. Butcher, *J. Cryst. Growth* **269**, vii (2004).

³I. Vurgaftman and J. R. Meyer, *J. Appl. Phys.* **94**, 3675 (2003).

⁴M. Cardona and N. E. Christensen, *Solid State Commun.* **116**, 421 (2000).

⁵See e.g., A. Punnoose and A. M. Finkel'stein, *Phys. Rev. Lett.* **96**, 057202 (2006).

⁶P. A. Lee and T. V. Ramakrishnan, *Rev. Mod. Phys.* **57**, 287 (1985).

⁷G. Bergman, *Phys. Rep.* **107**, 1 (1984).

⁸T. V. Shubina, S. V. Ivanov, V. N. Jmerik, D. D. Solnyshkov, V. A. Vekshin, P. S. Kop'ev, A. Vasson, J. Leymarie, A. Kavokin, H. Amano, K. Shimono, A. Kasic, and B. Monemar, *Phys. Rev. Lett.* **92**, 117407 (2004).

⁹T. Inushima, M. Higashiwaki, T. Matsui, T. Takenobu, and M. Motokawa, *Phys. Rev. B* **72**, 085210 (2005).

¹⁰J. J. Lin and J. P. Bird, *J. Phys.: Condens. Matter* **14**, R501 (2002).

¹¹X. D. Pu, J. Chen, W. Z. Shen, H. Ogawa, and Q. X. Guo, *J. Appl. Phys.* **98**, 033527 (2005).

¹²B. L. Altshuler, A. G. Aronov, D. E. Khmel'nitskii, and A. I. Larkin, in *Quantum Theory of Solids*, edited by I. M. Lifshits (Mir, Moscow, 1982), pp. 130–237.

¹³S. P. Fu and Y. F. Chen, *Appl. Phys. Lett.* **85**, 1523 (2004).

¹⁴P. Mohanty, E. M. Q. Jariwala, and R. A. Webb, *Phys. Rev. Lett.* **78**, 3366 (1997).

¹⁵A. Zawadowski, Jan von Delft, and D. C. Ralph, *Phys. Rev. Lett.* **83**, 2632 (1999).

¹⁶Z. G. Qian, W. Z. Shen, H. Ogawa, and Q. X. Guo, *J. Appl. Phys.* **93**, 2643 (2003).

¹⁷P. Parayanthal and F. H. Pollak, *Phys. Rev. Lett.* **52**, 1822 (1984).

¹⁸H. Richter, Z. P. Wang, and L. Ley, *Solid State Commun.* **39**, 625 (1981).

¹⁹I. H. Campbell and P. M. Fauchet, *Solid State Commun.* **58**, 739 (1986).